Design, Fabrication and Measurement of a Novel Compact Triband CPW-Fed Planar Monopole Antenna Using Multi-type Slots for Wireless Communication Applications

Ahmed Zakaria Manouare, Saida Ibnyaich, Divitha Seetharamdoo, Abdelaziz El Idrissi, Abdelilah Ghammaz

Accepted Manuscript

Journal of Circuits, Systems and Computers

Article Title:	Design, Fabrication and Measurement of a Novel Compact Triband CPW-Fed Planar Monopole Antenna Using Multi-type Slots for Wireless Communication Applications
Author(s):	Ahmed Zakaria Manouare, Saida Ibnyaich, Divitha Seetharamdoo, Abdelaziz El Idrissi, Abdelilah Ghammaz
DOI:	10.1142/S0218126620500322
Received:	19 September 2018
Accepted:	19 March 2019
To be cited as:	Ahmed Zakaria Manouare *et al.*, Design, Fabrication and Measurement of a Novel Compact Triband CPW-Fed Planar Monopole Antenna Using Multi-type Slots for Wireless Communication Applications, *Journal of Circuits, Systems and Computers*, doi: 10.1142/S0218126620500322
Link to final version:	https://doi.org/10.1142/S0218126620500322

Journal of Circuits, Systems, and Computers

Design, Fabrication and Measurement of a Novel Compact Triband CPW-Fed Planar Monopole Antenna Using Multi-type Slots for Wireless Communication Applications

Ahmed Zakaria Manouare*

Department of Applied Physics, Laboratory of Electrical Systems and Telecommunications LSET, FSTG
Cadi Ayyad University, Marrakesh 40000, Kingdom of Morocco
ahmedzakaria.manouare@gmail.com

Saida Ibnyaich

Department of Physics, I2SP Research Team, Faculty of Sciences Semlalia
Cadi Ayyad University, Marrakesh 40000, Kingdom of Morocco
ibnyaichsaida@gmail.com

Divitha Seetharamdoo

IFSTTAR, COSYS, LEOST Laboratory
Lille 1 University, 59650 Villeneuve d'Ascq, France
divitha.seetharamdoo@ifsttar.fr

Abdelaziz EL Idrissi and Abdelilah Ghammaz

Department of Applied Physics, LSET Laboratory, FSTG
Cadi Ayyad University, Marrakesh 40000, Kingdom of Morocco
az.elidrissi@gmail.com, aghammaz@yahoo.fr

Received (Day Month Year)
Revised (Day Month Year)
Accepted (Day Month Year)

A novel compact coplanar waveguide (CPW)-fed planar monopole antenna with triple-band operation is presented for simultaneously satisfying the LTE 2600, WiMAX, WLAN and X-band applications. It is printed on a single-layered FR4 substrate. In this paper, the proposed antenna, which occupies a small volume of 30 × 28 × 0.8 mm^3 including the ground plane, is simply composed of a CPW-fed monopole with U-, L-, and T-shaped slots. By carefully selecting the lengths and positions of both L-shaped and U-shaped slots, a good dual notched band characteristic at center-rejected frequencies of 3.10 GHz and 4.50 GHz can be achieved, respectively. The T-shaped slot is etched on the radiating element to excite a resonant frequency in the 7 GHz band. Then, to prove the validation of the typical design, a prototype model is fabricated and measured. The experimental result shows that the three frequency bands of 2.31–2.80 GHz (490 MHz), 3.37–3.84 GHz (470 MHz), and 5.04–7.94 GHz (2900 MHz) can successfully cover the desired bandwidths of LTE2600/WiMAX (3.50/5.50 GHz)/WLAN (5.20/5.80 GHz) and the X-band communication systems (7.1-GHz operation). The principal applications of the X-band are radar, aircraft, spacecraft and mobile or satellite communication system. Nearly omni-directional and bi-directional radiation patterns of the triband antenna are observed in both H- and E-planes, respectively. In addition, a reasonable gain over the operating bands has been obtained. Indeed, the

*Corresponding author.

good agreements between simulation and measurement results have validated the proposed structure confirming its potential for multiband wireless communication services.

Keywords: CPW-fed monopole antenna; compact antenna; triband; dual-band rejection function; L-shaped-slot; U-shaped slot; T-shaped slot; X-band; LTE2600/WiMAX/WLAN applications.

1. Introduction

With the fast development of wireless communication, the multifrequencies antenna which can cover multiple bands for different communication systems has become one of the most important circuit elements in all modern telecommunication devices. The Long Term Evolution (LTE 2600: 2.50–2.69 GHz), the Worldwide Interoperability for Microwave Access (WiMAX: 3.40–3.69 GHz and 5.25–5.85 GHz), the Wireless Local Area Network (WLAN) standards of both 5.15–5.35 GHz and 5.725–5.825 GHz (5.2/5.8-GHz operations) and the X-band satellite communication systems (7-GHz band) are the most popular applications in recent years. In order to satisfy the requirements of these aforementioned frequency bands for different standards simultaneously, multiband antennas with broad impedance bandwidth and excellent radiation performance are certainly required. As it is well known, many interests are focused on the design of planar monopole antennas for multiband wireless applications with characteristics of compact size, low profile, low manufacturing cost, light weight, ease of integration, sufficient bandwidth and good omni-directional radiation pattern. Obviously, multiband antennas are especially attractive. They not only take the task of multiband working, but also eliminate the need of two or more separate antennas, thus avoiding the isolation problem existing between various antennas. In addition, the coplanar waveguide (CPW) feed lines have some interesting advantages compared to microstrip feed lines such as: lower dispersion at high frequencies, uniplanar configuration (fabricated on a single metallic layer), broadband characteristics and ease of integration with active Monolithic Microwave Integrated Circuits (MMIC) devices.[1] There is a huge need to have a miniaturized antenna that supports multiple advanced wireless protocols. For this need, several techniques have been reported in the literature to realize multifrequency planar monopole antennas employing CPW feed.

A CPW-fed planar rectangular antenna with the improvement of the bandwidth using the slot technique is presented in Ref. 2. A slot-monopole antenna with embedded rectangular parasitic elements[3] and a coplanar waveguide (CPW)-fed rhombus slot antenna[4] for WLAN applications are proposed. In Ref. 5, the authors suggested modified radiating stub with a pair of hook-shaped slits and slotted ground plane for 1.8/1.9/2.3/3.5-GHz operations. In Ref. 6, by introducing a pair of straight strips and two etched ∩-shaped slots, the proposed rhombic slot antenna can operate in multibands for WLAN/WiMAX applications. A planar antenna with a compact radiator for WLAN operation is reported in Ref. 7. This antenna is composed of an L-shaped and E-shaped radiating elements to generate two resonant modes. A rectangular patch antenna for RFID and WLAN applications[8] and a coplanar waveguide (CPW)-fed printed monopole antenna with an n-shaped slot for PCS/CDMA2000/TD-SCDMA/WLAN operations[9] are

studied. In Ref. 10, Song et al. proposed coplanar waveguide (CPW)-fed triangle-shaped monopole antenna for WLAN and WiMAX bands, but sufficient bandwidth enhancement is not brought about in the lower band. The aperture-coupled stack antenna is configured for WLAN and WiMAX standards.[11] This antenna is composed of a square fractal patch (Minkowski-island-based fractal geometry) with aperture coupling which makes its structure much more complex. However, the majority of these antennas designs reported[2-11] till now exhibit a single-band [2] or dual-band[3-11] characteristics.

In order to provide compatibility with more communication standards in a single device, a microstrip feed line, a substrate and a ground plane on which some simple slots are etched to achieve triband planar antenna for 2.4/5.2/5.8 GHz and 2.5/3.5/5.5 GHz applications simultaneously.[12] In Ref. 13, the triple frequency bands are excited by a square-slot antenna along with a pair of symmetrical L-strips and a monopole radiator for WLAN (2.4/5.2 GHz) and WiMAX (2.5/3.5 GHz) operations. A multiband monopole antenna with complementary split-ring resonators (CSRRs)[14] and a CPW-fed double rectangular ring-shaped monopole antenna with vertical slots in the ground plane to cover the entire WLAN/WiMAX wireless applications[15] are introduced. The antenna consisting of double C-shaped monopole strips and an inverted U-shaped shorted strip to generate three resonant modes and suitable for multifrequency operations is presented in Ref. 16. Furthermore, the triple-band feature can also be created by an asymmetric coplanar strip fed Sinc shaped structure[17] and an E-shaped printed antenna loaded with two narrow slots[18]. These antennas[12-18] achieve a relatively compact size, but they fail to cover 7 GHz frequency band to satisfy the X-band satellite communication requirement. In Ref. 19, the printed antenna which is composed of a rectangular ring, an S-shaped strip, a crooked U-shaped strip and three straight strips has acceptable triple-band characteristics covering WLAN/WiMAX operations. Three different types of structures; namely two I-shaped notched slots, an open-ended U-shaped slot and two symmetrical meander microstrip-lines, were used to generate three operating bands for WiFi/WiMAX bands. [20] An antenna formed by multi-triangular structure as metal ground plane and the radiation element with four different branches for 2.45/2.5/3.5/5.8 applications is presented in Ref. 21. Unfortunately, although these three latter antennas exhibit good multiband performance, they are somewhat complicated in structure. In Ref. 22, a triband operation is obtained by inserting dual arc-shaped strips into a slot antenna. Nevertheless, the narrow impedance bandwidth, especially in the upper band, and the large size (75×75 mm^2) limit its availability for practical engineering applications. In Ref. 23, an asymmetric M-shaped patch is employed to design a multiband antenna, and vias on the longer arm of the patch are used for the purpose of improving the bandwidth. The H-shaped slot antenna fed by microstrip coupling to cover GPS and Wi-Fi applications is discussed in Ref. 24. Although these two latter structures could fulfill the communication demands of triple-band, they both suffer the disadvantage of big antenna dimensions.

Inspired by the band-notched ultrawideband (UWB) antenna[25-27], the operation of multiband can also be achieved through the introduction of various stopband rejections in a broad impedance bandwidth. For the reason of producing these notched bands without

raising the total size of the radiating antenna, etched half-wavelength slots are employed. Moreover, the excess coupling produced by the complex structure in Ref. 28 makes the antenna design difficult when multiple stopband rejections are needed. To overcome this issue, a new technique is developed in this work by the use of a special slot, whose length is only about a quarter of the guided wavelength at the desired notching frequency for triband wireless communication systems.

In the present paper, a novel triband CPW-fed planar monopole antenna is proposed. This compact antenna is designed to generate three separate operating bands of 2.31–2.80 GHz, 3.37–3.84 GHz and 5.04–7.94 GHz to satisfy the LTE 2600, WiMAX (3.50/5.50 GHz), WLAN (5.20/5.80 GHz) applications and the X-band satellite communication systems (7-GHz band). The proposed antenna of overall dimensions 30 × 28 mm^2 consists of three distinct slots that are integrated in a limited space of the wideband radiating patch to obtain multiband operation. The L-shaped and U-shaped slots which are of the length of about a quarter and a half of the guided wavelength respectively are combined to reject two undesired resonances at around 3.10 GHz and 4.50 GHz, respectively which makes antenna miniaturization possible. Therefore, these two slots are utilized to bring two notched bands without affecting the radiation performance of the antenna. The T-shaped slot is embedded on the monopole antenna to create an additional resonance frequency at 7 GHz band without modifying the performance of the other bands. It is also noticeable that the band-rejected property of the antenna is tunable. Details of the proposed antenna design are described and both the numerical and the experimental results are presented and analyzed as well.

The next parts of this paper are organized as follows: Section II discusses the geometry and the design guidelines of the proposed antenna structure. Section III presents the parametric studies of the key parameters of the proposed antenna. Section IV provides proofs that the proposed antenna is well suited for triband LTE2600/ WiMAX/ WLAN and X-band wireless communication applications with its simulated and measured results. Finally, a brief conclusion is given in Section V.

2. Antenna Design Principles

Figure 1 represents the configuration of the suggested monopole antenna with overall dimensions of only 30 (W) × 28 (L) mm^2. We designed our triband antenna with an FR4 (Flame Resistant 4) dielectric substrate on a thickness of H= 0.8 mm, a relative permittivity of ε_r= 4.2, a loss tangent of tanδ= 0.016 and a coppering thickness of the radiator t= 0.035 mm. To feed the antenna, we used a 50 Ω CPW transmission line that has a central strip having as width W_f and the gap distance between the central feed line and the coplanar ground plane is G. Both ground planes with similar dimensions of W_g × L_g were placed on each side of the CPW line. The radiating patch occupies a small size of W_{11} × L_{11} with U- and L-shaped slots formed by dimensions W_{31} × L_{31} and W_{41} × L_{41}, respectively. In our design, these two slots are used with a width of 0.4 mm (U shape) and 0.5 mm (L shape) to yield notched bands at certain frequencies that are related to their lengths. With the size of W_{51} × L_{51}, the T-shaped slot is etched on the right side of

the radiating element to produce a resonant frequency at higher band. To investigate the performance of the proposed antenna structure in terms of achieving multiband operations, a commercially available simulation software of CST Microwave Studio (CST MWS) based on Finite Integration Technique (FIT) was used for the required numerical analysis and to obtain the appropriate geometrical parameters which are listed in Table 1. The antenna design evolution process to achieve the triple-band operation for LTE 2600, WiMAX, WLAN and X-band applications can be divided into five steps with different antenna configurations which are denoted in Fig. 2 as Stage 1, Stage 2, Stage 3, Stage 4 and the Proposed antenna, respectively.

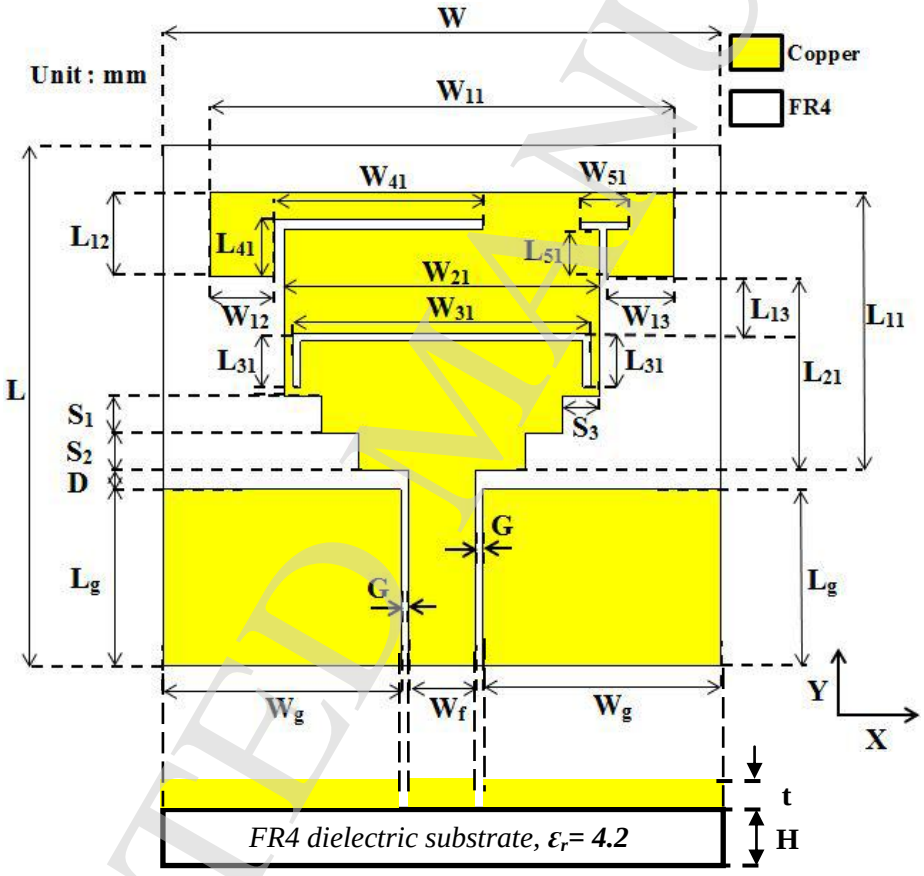

Fig. 1. Configuration of the proposed triband antenna.

The simulated results of reflection coefficient (S_{11}) carried out by Computer Simulation Technology (CST) Microwave Studio (MWS) are plotted in Fig. 3. First, the original CPW-fed monopole antenna consists of two elements: horizontal and vertical with dimensions of $W_{11} \times L_{12}$ and $W_{21} \times L_{21}$, respectively and a spacing of D= 1 mm away from the CPW ground (Stage 1 shown in Fig. 2(a)) so as to excite one resonant mode at 3.98 GHz. This frequency is mainly caused by the fundamental mode of the

antenna since it has a resonant path length of about 15 mm (i.e.= L_{12} + L_{21}), which is very close to one-quarter wavelength for operating at 3.98 GHz. A wide bandwidth of 3.41 GHz (from 3.12 to 6.53 GHz) defined by the $S_{11} \leq -10$ dB is obtained, as shown in Fig. 3. Second, the staircase patterns notched on the edges of the monopole antenna (Stage 2 depicted in Fig. 2(b)) play an important role to lead the resonant frequency of the mode at about 3.98 GHz to shift towards a lower frequency of 3.40 GHz since the surface current mode is mostly peripheral. Third, the effect of U-shaped slot etched on the radiating patch is depicted in Fig. 3 (Stage 3); we notice a generation of a notched band at around 4.50 GHz and a great improvement in the impedance matching at 5.45 GHz (S_{11}= -34.5 dB). Thus, the monopole antenna in this step produces two distinct bands ranging from 2.70 to 3.35 GHz (650 MHz) and from 5 to 6.81 GHz (1810 MHz) for the first and second bands, respectively with two resonances at about 2.98 GHz and 5.45 GHz. In order to satisfy the middle frequency for WiMAX application, an L-shaped slot is used in Stage 4 for the reason of generating a second notched band at about 3.10 GHz. Also, it changes the impedance characteristics nearby, making the impedance match near 3.50 GHz considerably improved. Consequently, the 3.50-GHz WiMAX band is easily covered without altering the antenna size. It should be noted that the antenna in Fig. 2(d) provided three operation bands of 2.48-2.77 GHz (290 MHz) centered at 2.62 GHz, 3.37-3.85 GHz (480 MHz) centered at 3.55 GHz and 5.04-6.9 GHz (1860 MHz) centered at 5.56 GHz. Finally, when the T-shaped slot is embedded into the right side of the planar monopole radiator, a new resonance at 7.10 GHz is excited and good triple-band features for $S_{11} \leq$ -10 dB are also obtained.

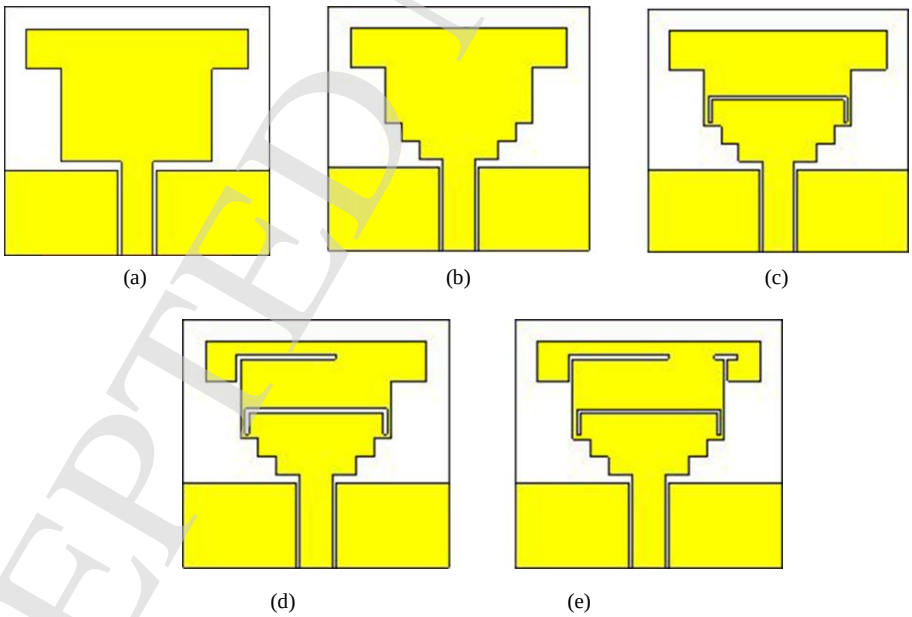

Fig. 2. Evolution process of the proposed CPW-fed triband antenna: (a) Stage 1, (b) Stage 2, (c) Stage 3, (d) Stage 4, (e) Proposed antenna.

The simulated result of reflection coefficient shown in Fig. 3 indicates that the proposed antenna in Fig. 2(e) has achieved broad operating bandwidths of 330 MHz (2.47–2.80 GHz, f_{r1}= 2.63 GHz), 460 MHz (3.37–3.83 GHz, f_{r2}= 3.53 GHz) and 2740 MHz (5.04–7.78 GHz, f_{r3}= 5.56 GHz / f_{r4}= 7.10 GHz), fully covering the LTE 2600 (2.50–2.69 GHz), 3.50/5.50-GHz WiMAX (3.40–3.69 GHz and 5.25–5.85 GHz), 5.20/5.80-GHz WLAN (5.15–5.35 GHz and 5.725–5.825 GHz) applications and the X-band satellite communication systems (7-GHz band).

Table 1. Optimal design parameters of the proposed triband antenna (Unit: mm).

Parameters	Dimensions (mm)	Parameters	Dimensions (mm)
W	30	W_{41}	11.2
L	28	L_{41}	3
W_{11}	25	W_{51}	2.6
L_{11}	15	L_{51}	2.5
W_{12}	3.5	S_1	2
L_{12}	4.5	S_2	2
W_{13}	3.6	S_3	2
L_{13}	3.1	W_g	12.8
W_{21}	17	L_g	9.5
L_{21}	10.5	W_f	3.6
W_{31}	16	G	0.4
L_{31}	2.5	D	1

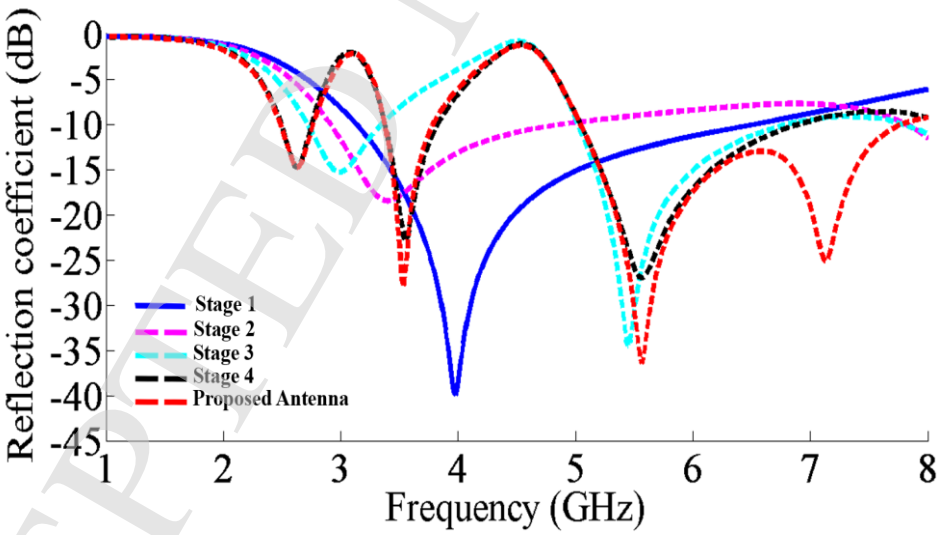

Fig. 3. Reflection coefficient with respect to frequency for the antenna design stages and the optimal triband antenna configuration.

It is important to mention that the two center-rejected frequencies, f_1 and f_2, for the stopbands may be empirically approximated by:

$$f_1 = \frac{C}{4 \times L_{s1} \times \sqrt{\varepsilon_{reff}}} \quad (1)$$

$$f_2 = \frac{C}{2 \times L_{s2} \times \sqrt{\varepsilon_{reff}}} \quad (2)$$

$$\varepsilon_{reff} \approx \frac{\varepsilon_r + 1}{2} \quad (3)$$

Where C is the speed of light in free space, ε_r is the relative permittivity of the substrate and ε_{reff} is the effective relative permittivity. From the antenna geometry (Fig. 1) and the optimized dimensions specified in Table 1, the two resonant lengths L_{S1} and L_{S2} can be determined by:

$$L_{s1} = W_{41} + L_{41} \quad (4)$$

$$L_{s2} = W_{31} + (2 \times L_{31}) \quad (5)$$

According to the formulas (1) to (5), we remark that the total lengths of the L-shaped and U-shaped slots can be evaluated to be L_{S1}= 14.2 mm (about a quarter of the guided wavelength) and L_{S2}= 21 mm (about a half of the guided wavelength), which correspond to the center-rejected frequencies at 3.10 GHz and 4.50 GHz, respectively. Likewise, by using the aforementioned equations, the L_{S1} and L_{S2} of the two slots are calculated and mentioned along with the simulated values in Table 2. It is clearly seen that these calculated values are quite close to those simulated.

Table 2. Comparison between simulated and calculated total length of the L-shaped and U-shaped slots.

Rejected Frequency	**Total Length of the Slot**		
	Length	**Calculated value**	**Simulated value**
f_1= 3.10 GHz	L_{S1}	15 mm	14.20 mm
f_2= 4.50 GHz	L_{S2}	20.67 mm	21 mm

The simulated voltage standing wave ratio (VSWR) for various antenna design stages illustrated in Fig. 2 is demonstrated in Fig. 4. The first curve (Stage 1) corresponds to the response of the reference broadband antenna. The bandwidth ranges from 3.12 to 6.53 GHz (3.41 GHz) for a VSWR less than 2. In Stage 2, the original resonance (at 3.98 GHz) is definitely moved towards the lower frequency (at 3.40 GHz) due to the resonant current path which is lengthened. It is also observed that the obtained band-notched characteristic is very close to the center-rejected frequency of 4.50 GHz when the U-shaped slot is inserted in Stage 3. By employing an L-shaped slot, an additional band-stop at center-rejected frequency of 3.10 GHz is created as shown in Stage 4. For the proposed antenna, the variation of the VSWR according to frequency shows that it is inferior to 2 except for the two notched frequency bands 2.81–3.36 GHz and 3.84–5.03 GHz. It can be noticed from the plot that the value of the VSWR is approximately 8 at 3.10 GHz and 13.32 at 4.50 GHz. Therefore, a good matching condition in the three operating frequency bands is remarked.

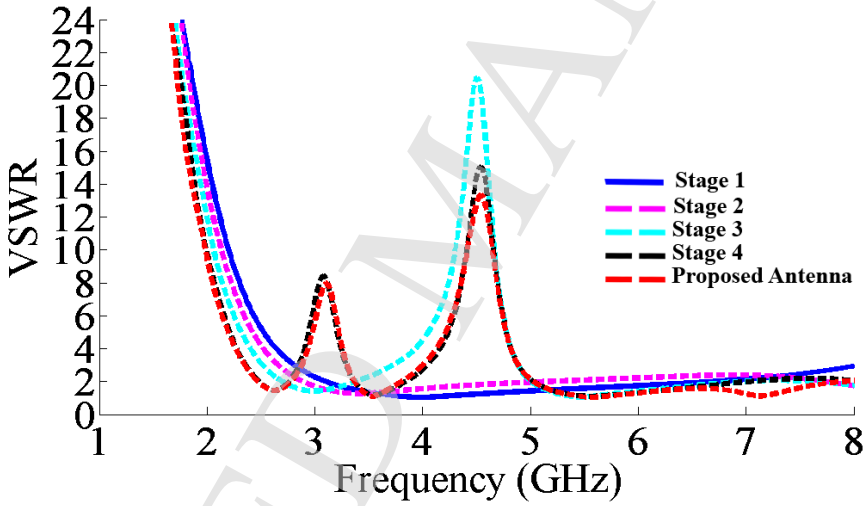

Fig. 4. Simulated VSWR for the different antenna structures generated in the evolution process.

To further study the dual stopband rejection property of the antenna, here we also simulate the surface current distributions on the radiation patch of proposed triband antenna for the center-rejected frequencies at about 3.10 GHz and 4.50 GHz, respectively and the resonant frequency at 7.10 GHz. As expected, when the antenna works at 3.10 GHz, a strong resonant current shown in Fig. 5(a) flows along the L-shaped slot to generate the first stopband, but nearly no current on the other embedded slots. This demonstrates that the first notched band is produced by the L-shaped slot (quarter-wavelength slot). A similar result is observed in Fig. 5(b), the resonant currents at rejected frequency 4.50 GHz are effectively distributed on the U-shaped slot. It is evident that the second stopband is excited mainly due to the U-shaped slot (half-wavelength slot). Figure 5(c) reveals the distribution of the surface currents at a passband frequency of 7.10 GHz. For this latter resonant frequency, most of the surface currents are

concentrated along the T-shaped slot at the right side of the radiating patch monopole indicating that this slot is responsible for generating the 7-GHz band; and it does not contribute to the notched frequency band response at 3.10 GHz and 4.50 GHz. These simulations clearly validate our design concept of the proposed antenna.

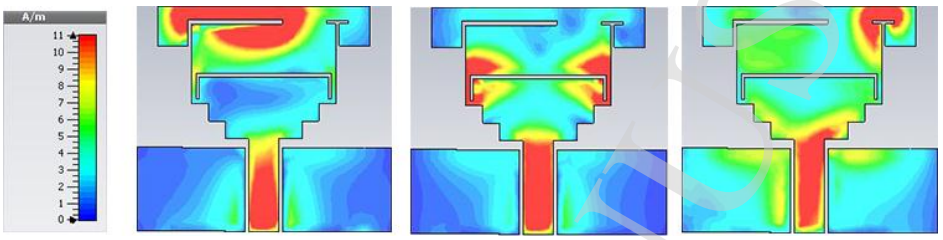

(a) (b) (c)

Fig. 5. Simulated surface current distributions at various frequencies of the proposed antenna: (a) 3.10 GHz, (b) 4.50 GHz, (c) 7.10 GHz.

To understand the influence of the different dimensions namely W_{12}, W_{13}, L_{13}, L_{51} and total lengths of both the L-shaped slot (L_{S1}) and the U-shaped slot (L_{S2}) on reflection coefficient (S_{11}) result, a parametric study on the triple-band planar monopole antenna is carried out in the following section.

3. Parametric Study

In this final antenna design, the first band (2.47–2.80 GHz), the second band (3.37–3.83 GHz) and the third band (5.04–7.78 GHz) are obtained mainly because of the use of the CPW-fed planar monopole radiator with U-, L-, and T-shaped slots. The performance of the antenna is affected by several parameters. Therefore, effects of the key structure parameters, including the lengths and positions of the multi-type slots on the notched bands are simulated and analyzed. This study is based on the proposed triband antenna shown in Fig. 1.

3.1. *Length of the three slots (variation of L_{S1}, L_{S2} and L_{51} parameters)*

This section discusses the variation of L_{S1} (the total length of the L-shaped slot), L_{S2} (the total length of the U-shaped slot) and L_{51} (the length of the T-shaped slot).

Figure 6 shows the reflection coefficient simulation results when the L_{S1} parameter was altered. It is observed that the first notched band can be controlled only by adjusting the length of the L-shaped slot. The resonance of the first rejected frequency shifts down from 3.43 GHz to 2.96 GHz as L_{S1} increases from 12.2 mm to 15.2 mm. The proper notched band of 0.55 GHz (from 2.81 GHz to 3.36 GHz) was obtained when the overall length of the L-shaped slot (L_{S1}= W_{41}+L_{41}) was 14.2 mm. This latter length was approximately a quarter of the guided wavelength, corresponding to equation (1). Although the variation of L_{S1} had no effect on the second notched band and the resonant frequency at 7-GHz band, there was a high effect on the impedance matching of the

second band for WiMAX 3.50-GHz application. As L_{S1} decreases with an interval of 1 mm, the middle resonant mode shifts towards a higher frequency (from 3.44 GHz to 3.80 GHz) and the reflection coefficient is importantly decreased (S_{11}= -16.6 dB) for value L_{S1}= 12.2 mm. We notice that the main function of the L-shaped slot is to produce the first notched band at center-rejected frequency of 3.10 GHz and also to achieve a good impedance matching in the second operating band.

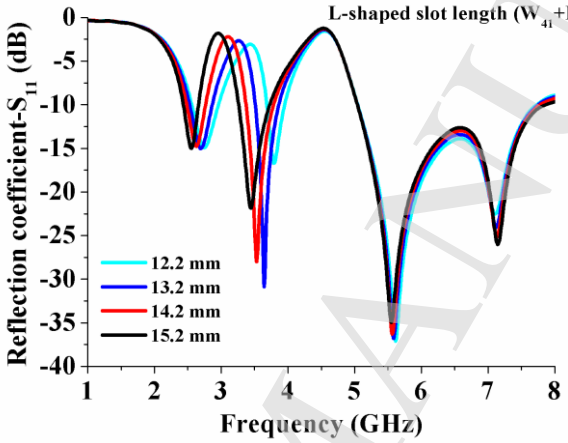

Fig. 6. Reflection coefficient (S_{11}) with respect to frequency for various values of L_{S1}; other parameters are the same as listed in Table 1.

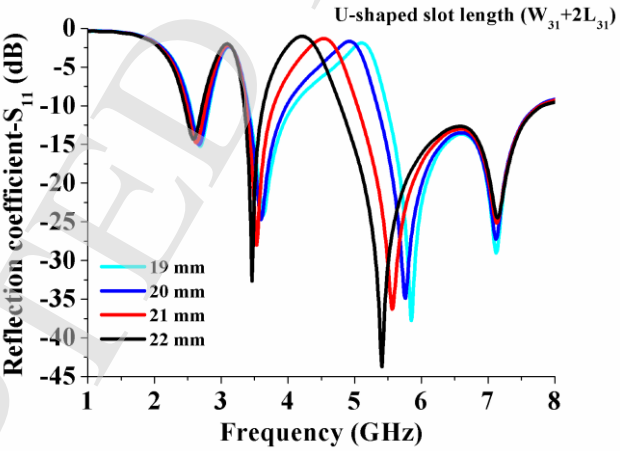

Fig. 7. Reflection coefficient (S_{11}) with respect to frequency for various values of L_{S2}; other parameters are the same as listed in Table 1.

Figure 7 shows the reflection coefficient simulation results when the length of the U-shaped slot denoted by L_{S2} parameter was varied. The antenna uses this slot with different

lengths from 19 mm to 22 mm to reach a tunable center-rejected frequency range from 5.10 GHz to 4.22 GHz for the second notched band. There was no effect on the first notched band and the resonant mode at upper frequency band (7.10-GHz operation). At the length L_{S2}= 21 mm which is chosen as an optimum value, the notched band of 1.19 GHz with a frequency range from 3.84 GHz to 5.03 GHz at center-rejected frequency 4.50 GHz was obtained. In addition, the total length of the U-shaped slot (W_{31}+2×L_{31}= 21 mm) was approximately a half of the guided wavelength of the frequency of 4.50 GHz (equation (2)). On the other hand, by increasing this length, the third resonant mode shifts towards a lower frequency (from 5.85 GHz to 5.41 GHz) with an improvement in the impedance matching. Therefore, it can be concluded that the second notched band can be controlled in an efficient manner by tuning the dimension L_{S2} (W_{31}, L_{31}) of the U-shaped slot.

Figure 8 depicts the variation of the reflection coefficient against frequency for various values of L_{51} while keeping all the other parameters unchangeable. As evident from the figure, when the dimension of L_{51} increases from 2 mm to 3.5 mm with a step of 0.5 mm, the resonant mode at 7-GHz band shifts towards a lower frequency from 7.51 GHz to 6.38 GHz without modifying the properties of the dual notched bands at center-rejected frequencies of 3.10 GHz and 4.50 GHz. Thus, the value of L_{51} is chosen 2.5 mm as optimum to excite the frequency 7.10 GHz. By changing this length, we remark that the first and second bands remain unaltered. It should be also noted that the T-shaped slot has a significant effect solely on the higher resonant mode for X-band application.

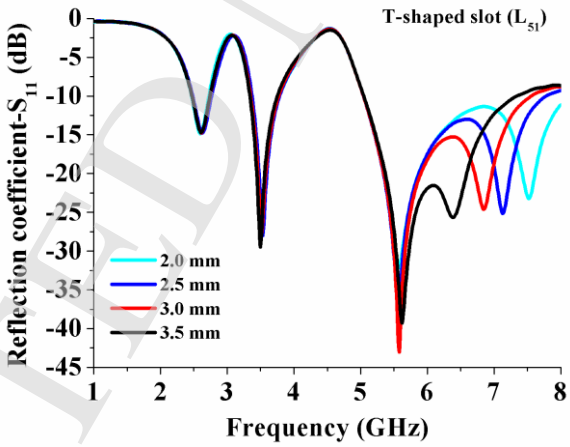

Fig. 8. Reflection coefficient (S_{11}) with respect to frequency for various values of L_{51}; other parameters are the same as listed in Table 1.

3.2. *Position of the three slots (variation of W_{12}, L_{13} and W_{13} parameters)*

As mentioned, the rejected frequencies and notched bandwidths of the proposed antenna were varied with respect to the lengths of both L-shaped and U-shaped slots. The T-

shaped slot was adopted to create a resonant frequency at 7-GHz band (the upper frequency band of the planar triband antenna becomes wider). However, their positions also affected the antenna characteristics. Figure 9 illustrates the simulated results of the reflection coefficient (S_{11}) when the position of the L-shaped slot denoted by W_{12} parameter was changed. It was found that this parameter had greater effects on the first notched band but there were no effects on the others. It was also seen that when W_{12} was decreased from 3.5 mm to 0.5 mm, the level of S_{11} was increased from -25 dB to -34 dB at 7.10-GHz operation due to the changing of the electromagnetic coupling between the L-shaped and T-shaped slots. Additionally, by decreasing the width W_{12}, the first rejected frequency of 3.10 GHz shifted to a higher frequency and vice versa.

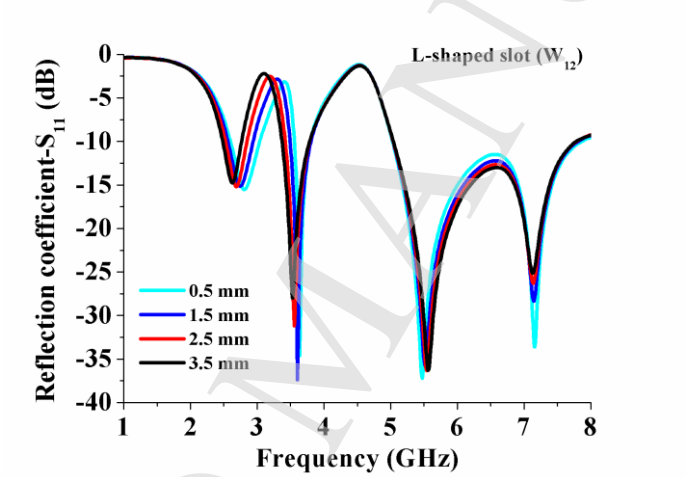

Fig. 9. Reflection coefficient (S_{11}) with respect to frequency for various values of W_{12}; other parameters are the same as listed in Table 1.

As indicated in Fig. 10, the position of the U-shaped slot has a major impact on bandwidth of the second notched frequency band. The results show that when the dimension L_{13} was increased from 0.7 mm to 3.1 mm with an interval of 0.8 mm, the bandwidth of the second notched frequency has broadened from 0.8 GHz (4.05-4.85 GHz) to 1.19 GHz (3.84-5.03 GHz). As well, the reflection coefficient was raised in the 5-GHz band with a shifting of the resonant frequency from 5.20 GHz to 5.56 GHz, whereas the first notched band at center-rejected frequency of 3.10 GHz keeps almost unchanged. On the other hand, we notice also a variation in the level of S_{11} for the 7-GHz band which is possibly due to the changing coupling between the U-shaped and T-shaped slots.

The simulated reflection coefficient (S_{11}) for various values of the width W_{13} has been plotted in Fig. 11. The results indicate that the highest resonant mode of the proposed antenna can be effectively controlled by adjusting the position of the T-shaped slot (W_{13} parameter). The resonant mode at 7-GHz band shifts toward a higher frequency side (from 7.10 GHz to 7.72 GHz) due to the decrement of the dimension W_{13} from 3.6 mm to

1.2 mm. At the same time, there is no significant change in the two notched bands at center-rejected frequencies of 3.10 GHz and 4.50 GHz. Hence, the value of W_{13} is selected to be 3.6 mm to achieve the 7.10-GHz application.

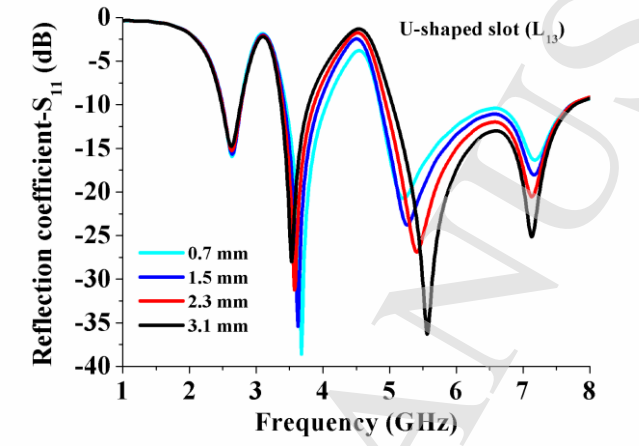

Fig. 10. Reflection coefficient (S_{11}) with respect to frequency for various values of L_{13}; other parameters are the same as listed in Table 1.

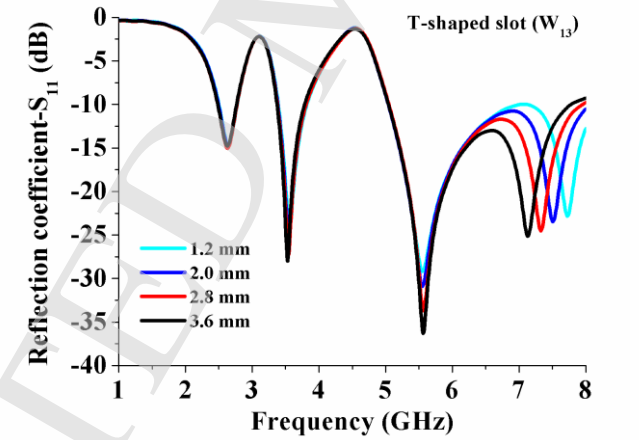

Fig. 11. Reflection coefficient (S_{11}) with respect to frequency for various values of W_{13}; other parameters are the same as listed in Table 1.

During the process of the parametric study above, it is obviously found that the center frequency and bandwidth of the notched band at 3.10 GHz and 4.50 GHz are mainly determined by the length and position of the L-shaped and U-shaped slots, respectively. Moreover, we can find out that by adjusting one parameter, only the corresponding notched frequency band changes while the other one is not affected. It is interesting to

note that it is possible to excellently tune and control the two rejected frequencies independently. Therefore, our proposed antenna has stable band-notched characteristics. By varying the two parameters L_{51} and W_{13}, the results demonstrate that the resonant frequency at 7.10 GHz is very sensitive to these dimensions. Thus, the T-shaped slot is primarily employed to operate at 7-GHz band (X-band application).

4. Results and Discussion

4.1. *Reflection coefficient results*

Both the CST Microwave Studio and the Ansoft High Frequency Structure Simulator HFSS based on Finite Element Method (FEM) are used to simulate the planar triband monopole antenna. In relation with the optimal dimensions revealed in Table 1, a prototype antenna is fabricated and experimentally characterized to verify the design concept as well as to validate the simulation results. In fact, the developed configuration was made on an FR4-epoxy substrate with a permittivity of ε_r= 4.2, a thickness of H= 0.8 mm, a loss tangent of tanδ= 0.016 and a 35 μm of metallization thickness. The SMA female connector is used for feeding with characteristic impedance of 50 Ω. The photograph of the prototype is presented in Fig. 12(a). The proposed antenna in anechoic chamber is shown in Fig. 12(b). Then, the measurement of the reflection coefficient (S_{11}) of this miniaturized triband antenna was carried out with Hewlett-Packard HP 8720D vector network analyzer, which has a frequency range limited to 20 GHz. The S_{11}-parameter was measured and the obtained result together with the simulated one are shown in Fig. 13. It can be observed that the simulated and measured results display an excellent agreement.

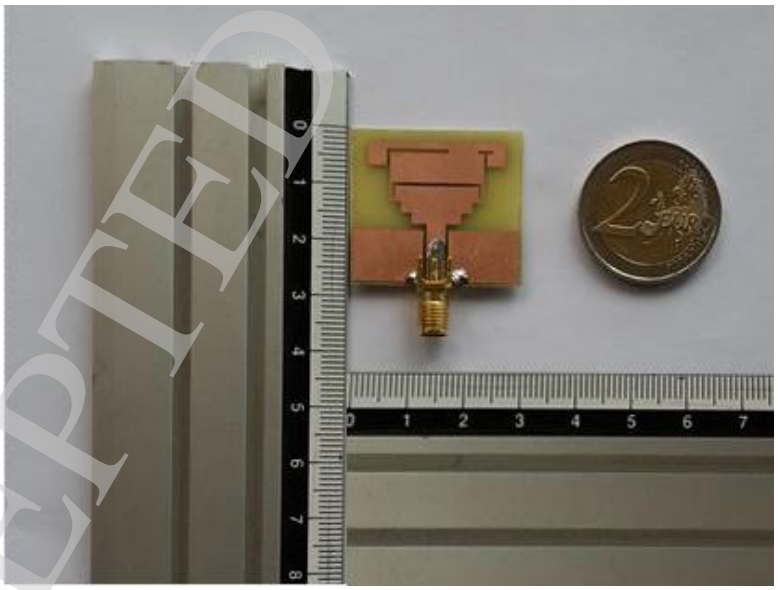

(a)

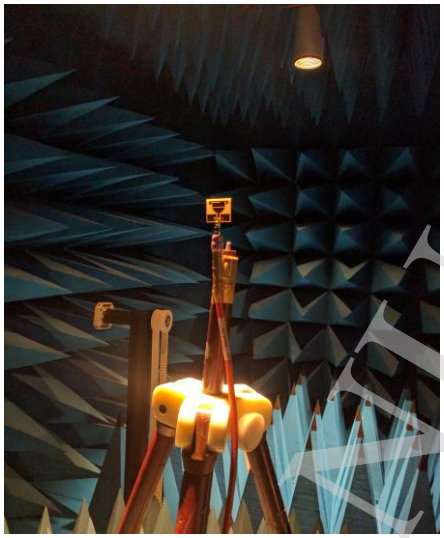

(b)

Fig. 12. (a) Photograph of the fabricated antenna, (b) proposed antenna in anechoic chamber.

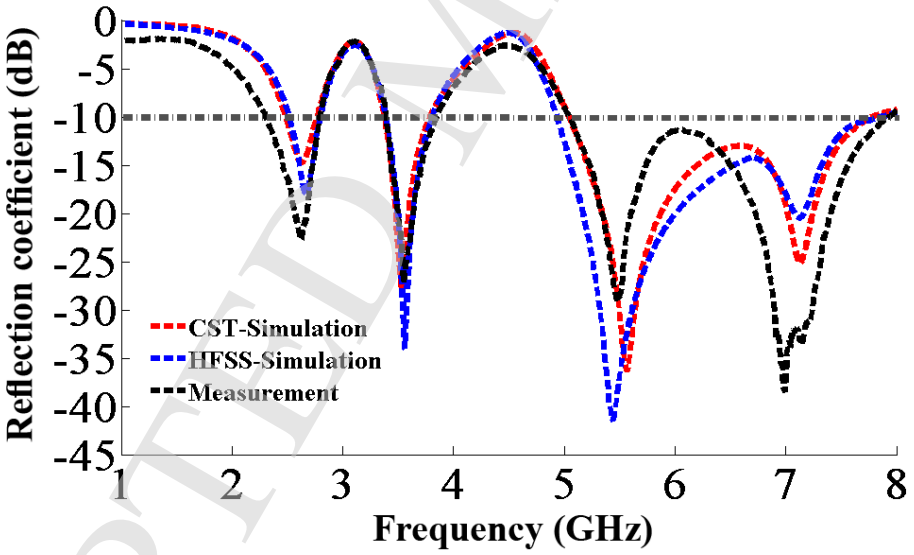

Fig. 13. Measured and simulated results of the reflection coefficient (S_{11}) with respect to frequency for the proposed triband antenna.

According to the experimental result, it is found that the proposed compact antenna can effectively cover three separate impedance bandwidths (for $S_{11} \leq$ -10 dB) of 490 MHz (2.31–2.80 GHz, f_{r1}= 2.62 GHz), 470 MHz (3.37–3.84 GHz, f_{r2}= 3.55 GHz), and 2900 MHz (5.04–7.94 GHz, f_{r3}= 5.47 GHz and f_{r4}= 7 GHz) which allow to better satisfy the LTE2600/ WiMAX (3.50/5.50 GHz)/ WLAN (5.20/5.80 GHz) applications and the X-

band satellite communication systems (7.10-GHz operation). For the fulfilled prototype antenna, it was proved that the desired operating bands are successfully excited with a good impedance matching for heterogeneous wireless communication systems.

Table 3 compares the measured and simulated results of the impedance bandwidths of the proposed antenna. These results coincide with each other and we notice that there is a sufficient bandwidth at the three frequency bands to cover the entire multi-standards LTE 2600, WiMAX, WLAN and X-band (7-GHz band) wireless applications.

Table 3. Comparison between measured and simulated impedance bandwidths of the proposed triband antenna.

	CST-Simulation	**HFSS-Simulation**	**Measurement**
First band	2.47-2.80 GHz (BW_1= 330 MHz) 12.54%	2.50-2.80 GHz (BW_1= 300 MHz) 11.27%	2.31-2.80 GHz (BW_1= 490 MHz) 18.70%
Second band	3.37-3.83 GHz (BW_2= 460 MHz) 13.03%	3.37-3.83 GHz (BW_2= 460 MHz) 12.95%	3.37-3.84 GHz (BW_2= 470 MHz) 13.23%
Third band	5.04-7.78 GHz (BW_3= 2740 MHz) 49.28%	5-7.86 GHz (BW_3= 2860 MHz) 52.57%	5.04-7.94 GHz (BW_3= 2900 MHz) 53.01%
Resonant frequencies (f_r) **Level reflection coefficients (S_{11})**	f_{r1}= 2.63 GHz S_{11}= -14.8 dB f_{r2}= 3.53 GHz S_{11}= -28.1 dB f_{r3}= 5.56 GHz S_{11}= -36.4 dB f_{r4}= 7.10 GHz S_{11}= -25.1 dB	f_{r1}= 2.66 GHz S_{11}= -17.9 dB f_{r2}= 3.55 GHz S_{11}= -34.1 dB f_{r3}= 5.44 GHz S_{11}= -41.4 dB f_{r4}= 7.11 GHz S_{11}= -20.4 dB	f_{r1}= 2.62 GHz S_{11}= -22.7 dB f_{r2}= 3.55 GHz S_{11}= -27.2 dB f_{r3}= 5.47 GHz S_{11}= -29.1 dB f_{r4}= 7.00 GHz S_{11}= -38.5 dB

4.2. *Radiation patterns results*

Figure 14 demonstrates the measurement and simulation of the radiation patterns in E-plane (YZ plane) and H-plane (XZ plane) for the frequencies of 2.60 GHz, 3.50 GHz, 5.50 GHz and 7 GHz, respectively. The obtained results show that fairly good omni-directional patterns are attained in the H-plane over the operating bands, and the patterns in the E-plane are almost bi-directional. It is also worth saying that there is a good agreement between measurement and simulation.

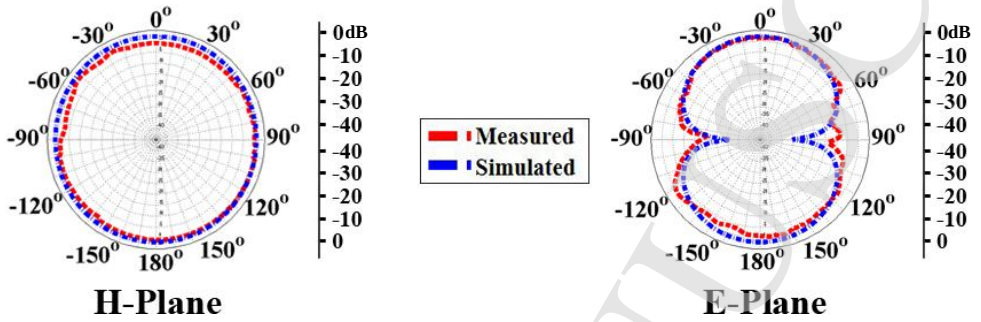

(a)

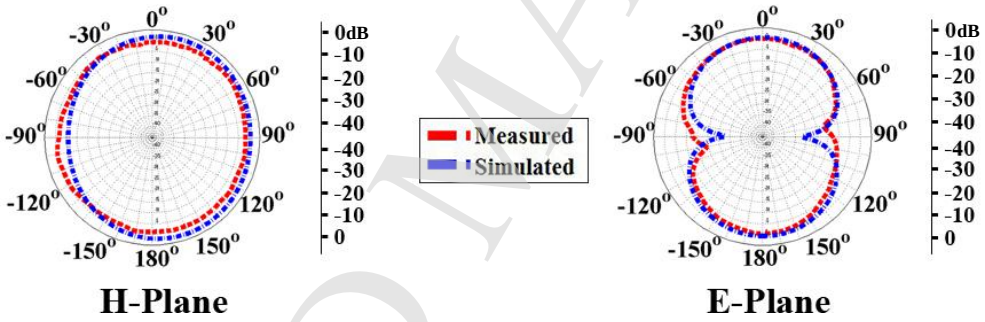

(b)

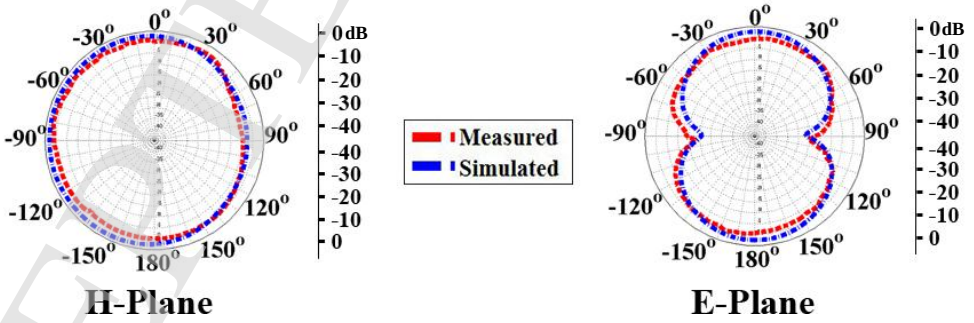

(c)

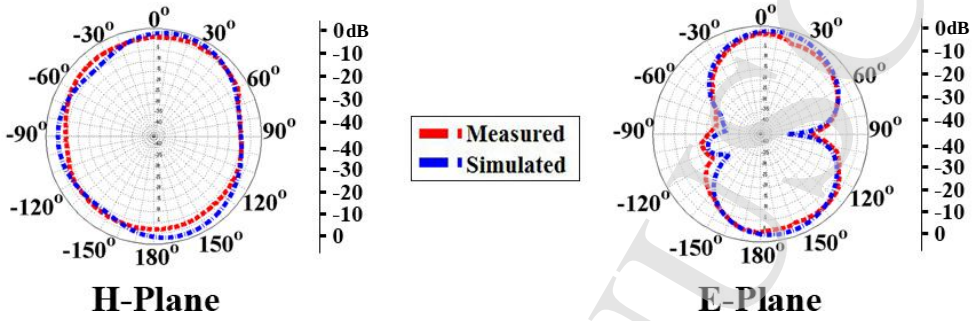

(d)

Fig. 14. Comparison between simulated and measured radiation patterns of the proposed antenna at frequencies: (a) 2.60 GHz, (b) 3.50 GHz, (c) 5.50 GHz and (d) 7 GHz.

4.3. *Gain and efficiency of the proposed antenna*

Figure 15(a) displays the simulated and measured gain versus the frequency of the proposed antenna. It is revealed from this figure that the peak gain falls down below 0 dBi at the two notched bands. Indeed, two sharp dips in the measured gain at center-rejected frequencies 3.10 GHz and 4.50 GHz can be observed. For the 2.60-GHz LTE band, the maximum gain is about 2.88 dBi. The antenna gain for the 3.50-GHz WiMAX band is varied from 1.34 to 3.15 dBi. Over the frequency range of 5.15-7.95 GHz for 5.20/5.80-GHz WLAN, 5.50-GHz WiMAX and 7.10-GHz X-band wireless communication systems, the gain varies from 1.61 to 5.81 dBi.

The radiation efficiency across the three operating bands is also depicted in Fig. 15 (b). For the first resonant band (2.31-2.80 GHz), the efficiency is greater than 80%. In the second resonant band (3.37-3.84 GHz), the efficiency of the designed antenna lies in a range from 64.7% to 83.67%, while in the third resonant band (5.04-7.94 GHz), the efficiency variation lies between 71.52% and 85.4%. As seen in Fig. 15(b), the radiation efficiency drops drastically for frequencies 3.10 GHz and 4.50 GHz.

Consequently, both the peak gain and efficiency are still adequate with a good band-rejected property for the proposed compact triband antenna. This latter is well suited for the practical LTE2600/WiMAX/WLAN/X-band applications.

To evaluate the performance of the fabricated prototype antenna, a comparative study of some earlier published articles is summarized in Table 4 wherein size, total occupied area, peak gain, operating bands and the corresponding impedance bandwidth of the antenna are considered. We can obviously see from this table that the proposed antenna achieves good multiband characteristics while maintaining an extraordinarily compact size, only occupying 82%, 70%, 71%, 63% and 23% area of those triple-band antennas in

Refs. 14, 16, 17, 21 and 24 respectively. On the other hand, in terms of bandwidth the prototype antenna is capable of generating three wide operating bands of 2.31–2.80 GHz, 3.37–3.84 GHz and 5.04–7.94 GHz, fully meeting the requirements of 2.60-GHz LTE, 3.50/5.50-GHz WiMAX, 5.20/5.80-GHz WLAN and the X-band wireless communications. Compared to antennas in Refs. 2-24, the novel triband CPW-fed planar monopole antenna could cover the specified frequency band of 7 GHz (X-band), which is important for modern wireless applications, such as radar, aircraft, spacecraft and mobile or satellite communication system, while other antennas cannot. Therefore, our designed antenna offers three sufficient impedance bandwidths, which comply with the frequency needs of 2.6/3.5/5.2/5.5/5.8/7.1 GHz operations. Likewise, this simple structure exhibits a significant miniaturization in size, an independent rejected-frequency control feature and a satisfactory gain level (5.81 dBi at upper band).

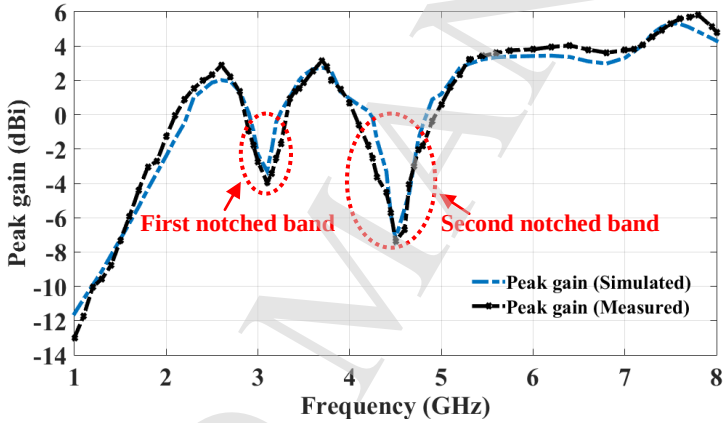

(a)

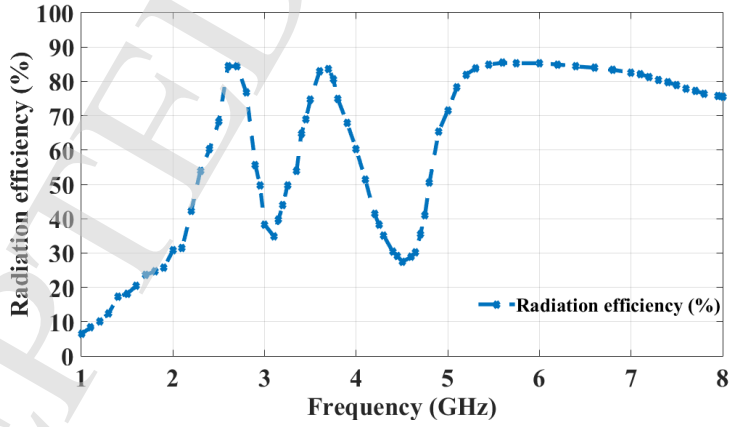

(b)

Fig. 15. (a) Peak gain and (b) radiation efficiency with respect to frequency for the proposed antenna.

Table 4. Performance comparison of the proposed antenna with other reported triband antennas.

Reference	Antenna size (mm × mm) (Total area occupied)	Frequency range (GHz)	Bandwidth (MHz)	Peak gain (dBi)	Frequency of operation (GHz)
[14]	30 × 34 (1020 mm^2)	2.3–2.6 3.3–3.7 5.1–5.5	300 400 400	-1 1 4	2.4/3.5/5.2
[16]	40 × 30 (1200 mm^2)	2.39–2.73 3.23–3.79 5.05–5.96	340 560 910	0.45 1.67 1.71	2.4/2.5/3.5 5.2/5.5/5.8
[17]	22 × 54 (1188 mm^2)	2.11–2.38 4.18–4.6 5.2–5.678	270 420 478	2.15 3.42 5.01	2.3/4.35/5.4
[21]	44 × 30 (1320 mm^2)	2.2–2.9 3.16–3.7 5.05–5.9	700 540 850	1.09 2.45 3.82	2.4/2.5/3.5/5.8
[24]	60 × 60 (3600 mm^2)	1.55–1.57 2.39–2.69 4.97–5.93	20 300 960	0.26 4 3.7	1.575/2.5/5.2/5.8
Proposed antenna	30 × 28 (840 mm^2)	2.31–2.80 3.37–3.84 5.04–7.94	490 470 2900	2.88 3.15 5.81	2.6/3.5/5.2 5.5/5.8/7.1

5. Conclusion

A novel compact CPW-fed planar monopole antenna operating in three distinct bands to cover different standards of LTE 2600 (4G), WiMAX operations 3.50/5.50 GHz, WLAN operations 5.20/5.80 GHz and the X-band satellite communication systems (7-GHz band) has been presented. In comparison to conventional structures, the miniature triband antenna of overall dimensions 30 × 28 mm^2 is easy to fabricate and only uses an L-shaped slot (quarter-wavelength slot) and a U-shaped slot (half-wavelength slot) in order to generate two individual notched bands at center-rejected frequencies of 3.10 GHz and 4.50 GHz, respectively. An optimal T-shaped slot is successfully engraved on the right of the radiating patch to widen the highest operating band towards the 7 GHz band. Experiments are performed to validate the design concept. The fabricated antenna prototype revealed that there is a good agreement between measurement and simulation of the results with a good matching in the frequency bands of interest and stable omni-directional radiation characteristics with credible gains. For these reasons, the proposed

antenna is a very good candidate for integration within various portable devices for multiband wireless communication applications.

Acknowledgments

The authors acknowledge funding from the regional REPONDES project and the ELSAT2020 project co-financed by the European Union with the European Regional Development Funds, the French state and the Hauts de France Region Council. In addition, this work was supported by the National Center for Scientific and Technical Research (CNRST-I 003/032) and the Ministry of Higher Education of Morocco.

References

1. M. Naser-Moghadasi, A. Danideh, A. Bakhtiari and R. Sadeghifakhr, Compact slot antenna for MIMO applications in the WLAN bands, *Microw. Opt. Technol. Lett*. **55** (2013) 2490–2493.
2. R. Dakir, J. Zbitou, A. Mouhsen, A. Tribak, A. Sanchez and M. Latrach, New low-cost broadband CPW-fed planar antenna, *Int. J. Microw. Wirel. Technol*. **8** (2016) 271–276.
3. C.-Y. Huang and E.-Z. Yu, A slot-monopole antenna for dual-band WLAN applications, *IEEE Antennas Wirel. Propag. Lett*. **10** (2011) 500–502.
4. C.-C. Lin, E.-Z. Yu and C.-Y. Huang, Dual-band rhombus slot antenna fed by CPW for WLAN applications, *IEEE Antennas Wirel. Propag. Lett*. **11** (2012) 362–364.
5. N. Ojaroudi and N. Ghadimi, Dual-band CPW-fed slot antenna with a pair of hook-shaped slits, *Microw. Opt. Technol. Lett*. **57** (2015) 172–174.
6. J.-J. Xie, X.-S. Ren, Y.-Z. Yin and S.-L. Zuo, Rhombic slot antenna design with a pair of straight strips and two ∩-shaped slots for WLAN/WiMAX applications, *Microw. Opt. Technol. Lett*. **54** (2012) 1466–1469.
7. X. L. Sun, L. Liu, S. W. Cheung and T. I. Yuk, Dual-band antenna with compact radiator for 2.4/5.2/5.8 GHz WLAN applications, *IEEE Trans. Antennas Propag*. **60** (2012) 5924–5931.
8. R. Karli and H. Ammor, Rectangular patch antenna for dual-band RFID and WLAN applications, *Wirel. Pers. Commun*. **83** (2015) 995–1007.
9. S. T. Fan, Y. Z. Yin, W. Hu, K. Song and B. Li, Novel CPW-fed printed monopole antenna with an n-shaped slot for dual-band operations, *Microw. Opt. Technol. Lett*. **54** (2012) 240–242.
10. Y. Song, Y. C. Jiao, G. Zhao and F. S. Zhang, Multiband CPW-fed triangle-shaped monopole antenna for wireless applications, *Prog. Electromagn. Res*. **70** (2007) 329–336.
11. T.-F. Hung, J.-C. Liu, C.-Y. Wei, C.-C. Chen and S.-S. Bor, Dual-band circularly polarized aperture-coupled stack antenna with fractal patch for WLAN and WiMAX applications, *Int. J. RF Microw. Comput. Aided Eng*. **24** (2014) 130–138.
12. L. Dang, Z. Y. Lei, Y. J. Xie, G. L. Ning and J. Fan, A compact microstrip slot triple-band antenna for WLAN/WiMAX applications, *IEEE Antennas Wirel. Propag. Lett*. **9** (2010) 1178–1181.
13. W. Hu, Y.-Z. Yin, P. Fei and X. Yang, Compact triband square-slot antenna with symmetrical L-strips for WLAN/WiMAX applications, *IEEE Antennas Wirel. Propag. Lett*. **10** (2011) 462–465.
14. S. C. Basaran, U. Olgun and K. Sertel, Multiband monopole antenna with complementary split-ring resonators for WLAN and WiMAX applications, *Electron. Lett*. **49** (2013) 636–638.
15. S. Jo, H. Choi, J. Lim, B. Shin, S. Oh and J. Lee, A CPW-fed monopole antenna with double rectangular rings and vertical slots in the ground plane for WLAN/WiMAX applications, *Int. J. Antennas Propag*. **2015** (2015) 1–7, doi: 10.1155/2015/165270.

16. L. Kang, X.-H. Wang, H. Li and X.-W. Shi, Planar monopole antenna with a compact radiator for tri-band applications, *Microw. Opt. Technol. Lett*. **57** (2015) 706–709.
17. R. K. Badhai and N. Gupta, Compact asymmetric coplanar strip fed Sinc shaped monopole antenna for multiband applications, *Int. J. Microw. Wirel. Technol*. **9** (2017) 205–211.
18. S. M. A. Nezhad and H. R. Hassani, A novel triband E-shaped printed monopole antenna for MIMO application, *IEEE Antennas Wirel. Propag. Lett*. **9** (2010) 576–579.
19. Y. Xu, Y.-C. Jiao and Y.-C. Luan, Compact CPW-fed printed monopole antenna with triple-band characteristics for WLAN/WiMAX applications, *Electron. Lett*. **48** (2012) 1519–1520.
20. P. Wang, G.-J. Wen, Y.-J. Huang and Y.-H. Sun, Compact CPW-fed planar monopole antenna with distinct triple bands for WiFi/WiMAX applications, *Electron. Lett*. **48** (2012) 357–359.
21. T. Yang, G. Wen, G. Jinsong and F. Xiaoguo, Compact multi-band printed antenna with multi-triangular ground plane for WLAN/WiMAX/RFID applications, *Int. J. Microw. Wirel. Technol*. **8** (2016) 277–281.
22. Y.-D. Wang, J.-H. Lu and H.-M. Hsiao, Novel design of semi-circular slot antenna with triple-band operation for WLAN/WIMAX communication, *Microw. Opt. Technol. Lett*. **50** (2008) 1531–1534.
23. L. Peng, C. -L. Ruan and X. -H. Wu, Design and operation of dual/triple-band asymmetric M-shaped microstrip patch antennas, *IEEE Antennas Wirel. Propag. Lett*. **9** (2010) 1069–1072.
24. T.-H. Chang and J.-Fu. Kiang, Compact multi-band H-shaped slot antenna, *IEEE Trans. Antennas Propag*. **61** (2013) 4345–4349.
25. J. Kazim, A. Bibi, M. Rauf, M. Tariq and Owais, A compact planar dual band-notched monopole antenna for UWB application, *Microw. Opt. Technol. Lett*. **56** (2014) 1095–1097.
26. A. Sohail, K. S. Alimgeer, A. Iftikhar, B. Ijaz, K. W. Kim and W. Mohyuddin, Dual notch band UWB antenna with improved notch characteristics, *Microw. Opt. Technol. Lett*., **60** (2018) 925–930.
27. W. Ali, A. A. Ibrahim and J. Machac, Compact size UWB monopole antenna with triple band-notches. *Radio Eng*., **26** (2017) 57–63.
28. S.-T. Fan, Y.-Z. Yin, H. Li, S.-J. Wei, X.-H. Li and L. Kang, A novel tri-band printed monopole antenna with an etched ∩-shaped slot and a parasitic ring resonator for WLAN and WiMAX applications, *Prog. Electromagn. Res. Lett*. **16** (2010) 61–68.